



# Novel Computational Approach to Solve Convolutional Integral Equations: Method of Sampling for One Dimension\*

Un nuevo enfoque computacional para solucionar ecuaciones integrales convolucionales: el método de muestreo para una dimensión

Date received: 9 March 2018 | Date approved: 7 March 2019 | Date published: 6 December 2019

**CARLOS IVÁN PÁEZ RUEDA**<sup>a</sup>

Pontificia Universidad Javeriana, Colombia  
ORCID: 0000-0003-1127-4843

**ROBERTO BUSTAMANTE MILLER**

Universidad de los Andes, Colombia  
ORCID: 0000-0003-4458-2551

\* Research article

This article is derived from the doctoral research of the first coauthor at the Universidad de los Andes, Colombia. That study was partially financed by the Plan de Formación Permanente del Profesor Javeriano (PFPP) from Pontificia Universidad Javeriana, Colombia.

<sup>a</sup> Corresponding author. E-mail: paez.carlos@javeriana.edu.co

DOI: <https://doi.org/10.11144/Javeriana.iyu23-2.ncas>

## How to cite this article:

C. I. Páez Rueda, and R. Bustamante Miller, "Novel computational approach to solve convolutional integral equations: Method of sampling for one dimension," *Ing. Univ.*, vol. 23, no. 2, 2019. <https://doi.org/10.11144/Javeriana.iyu23-2.ncas>

## Abstract

*Objective:* This paper proposes a new methodology to solve one-dimensional cases of integral equations with difference kernels using Fourier analysis. *Methodology:* In this study, it was proven that any Fredholm equation of the first kind can be expressed as an extended convolutional problem; consequently, a new approach to solve that problem, using the nonideal instantaneous sampling theory and Fourier analysis, can be developed. *Results and Discussion:* The proposal was extensively evaluated and compared with the method of moments by considering two benchmarks. The first was a narrowband problem related to a second-order differential equation with specific boundaries. The second was a standard wideband problem related to wire antenna radiation in electrodynamics, known as the Pocklington equation. In both cases, we derived new interpretations and different approaches to solve the problems efficiently. *Conclusions:* The new proposal generalized the method of moments via new interpretations, strategies and design rules. We found that the techniques based on the method of moments are point-matching procedures independent of the weighting functions; the basis functions can be designed as generalized interpolation functions with more information provided by the original domain; the weighting functions literally represent a sampled linear filter; the unknown continuous function can be approximated without using the classical variational approach; and several new strategies based on the Fourier transform can be used to reduce the computational cost.

**Keywords:** deconvolution, integral equations, method of moments, moment methods, sampling methods

## Resumen

*Objetivo:* Este artículo propone una nueva metodología para solucionar ecuaciones integrales conformadas con núcleos diferenciales de una dimensión usando el análisis de Fourier. *Metodología:* En este estudio, se ha probado que cualquier ecuación de Fredholm de primera clase puede ser expresado como un problema convolucional extendido; consecuentemente, un nuevo enfoque para solucionar ese problema, usando la teoría de muestreo instantánea no ideal y el análisis de Fourier, puede ser desarrollado. *Resultados y discusión:* La propuesta fue extensivamente evaluada y comparada con el Método de los Momentos usando dos benchmarks. El primero fue un problema de banda angosta relacionado con una ecuación diferencial de segundo orden con fronteras específicas. El segundo fue un problema estándar de banda ancha relacionada con la radiación de una antena de alambre en electrodinámica, denominado la Ecuación de Pocklington. En ambos casos, nuevas interpretaciones y diferentes enfoques fueron encontrados con el objeto de solucionar eficientemente los problemas. *Conclusiones:* La nueva propuesta generaliza el Método de los Momentos con nuevas interpretaciones, estrategias y reglas de diseño. Nosotros encontramos que las técnicas basadas en el método de los momentos son procedimientos de acople de puntos que independiente de las funciones de peso, las funciones base pueden ser diseñadas como funciones de interpolación generalizadas con más información provista por el dominio original; las funciones de peso literalmente representan a un filtro lineal muestreado; las funciones continuas desconocidas pueden ser aproximadas sin usar el enfoque variacional clásico; y varias nuevas estrategias basadas en la transformada de Fourier poder ser usadas para reducir el costo computacional.

**Palabras clave:** deconvolución, ecuaciones integrales, método de los momentos, métodos de muestreo

## **Main Nomenclature**

$g(x)$	Unknown function over the interval $[a, b]$ .
$f(x)$	Known function over the interval $[a, b]$ .
$K(x, u)$	Kernel of the integral equation.
$g_{\Omega}(x)$	Truncated function of $g(x)$ over the interval $x \in \mathbb{R}$ .
$f^{\infty}(x)$	Extended function of $f(x)$ over the interval $x \in \mathbb{R}$ .
$g_{\Omega}(x_n)$	Instantaneous value of $g_{\Omega}(x)$ at sample $x_n \in \mathbb{R}$ .
$\hat{g}_{\Omega}(x_n)$	Instantaneous approximation of $g_{\Omega}(x_n)$ .
$\Psi(x)$	Nonideal sampling function over the interval $x \in \mathbb{R}$ .
$\vartheta$	Sampling rate.
$p_n(x; \Delta)$	Generalized interpolation function over the interval $x \in \mathbb{R}$ .
$\tilde{h}(v)$	Fourier transform of $h(x)$ .
$\tilde{g}^{\Omega}(v)$	Fourier transform of $g_{\Omega}(x)$ .
$BW_2^h$	Essential bandwidth of $h \in L^2$ .
$L^{1 \wedge 2}$	Means $L^1 \cap L^2$ .

Mathematical definitions and other notations can be found in appendices A.1 and A.2.

## Introduction

Integral equations (IEs) allow the modeling of a large number of complex problems in several areas of engineering and physics such as heat and mass transfer, oscillation theory and electromagnetic fields. An IE is an equation in which an unknown function  $g(\cdot)$  related to an integral needs to be found under a known excitation  $f(\cdot)$ . Some examples include one-dimensional IEs with forms  $\exists g(\cdot): \int_a^b K(x, u)g(u)du = f(x)$  and  $\exists g(\cdot): \int_a^x K(x, u)g(u)du = f(x)$ , which are respectively known as the *Fredholm* and *Volterra equations* of the first kind, in which  $K(x, u)$  is usually known as the *kernel*.

Several techniques have been developed over the years to solve this kind of problem using exact, asymptotic and numerical approaches. A comprehensive summary of these techniques for different problems can be found in [1]–[3]. In particular, a well-known numerical technique to solve electromagnetic problems using IEs is called the *method of moments* (MoM) [4], [5]. This approach allows the development of a general framework including different types of modern techniques, known as the *method of weighted residuals* (MWR). For example, the *finite element method* (FEM) and the *finite difference method* (FDM) can be represented using the MWR [6], [7]. In recent times, the MoM has been used to solve multidimensional open boundary problems in electrodynamics, and it is included in many CAD platforms such as HFSS, IE3D, FEKO, and NEC.

In [8], we proposed an original approach to solve integral equations, based on the *nonideal instantaneous sampling theory*, which involved developing a novel framework for solving linear operators using *Fourier analysis*. The new approach was based on the fact that a Fredholm equation of the first kind with a *difference kernel*  $K(x, u) = K(x - u)$  can be expressed as an extended convolutional problem with form  $K(x) * g_\Omega(x) = f^\infty(x)$ , where  $g_\Omega(x)$  is a truncated function of  $g(x)$ ,  $f^\infty(x)$  is an extended function of  $f(x)$ ,  $\Omega \triangleq [a, b]$ , and  $(*)$  is the standard convolution operator. As a result, although the problem must be solved via matrix techniques using the original domain, the convolution properties and Fourier analysis can be used to design an efficient solution. This new property, known as the *convolutional equivalence*, allows the establishment of design rules that cannot be determined when using the MoM. These results are detailed in this paper through a new framework termed as the *method of sampling for one dimension* (MoS!-1D).

Most previous works aimed at solving Fredholm equations in the context of electrodynamics were focused mainly on the MoM. The different approaches established benchmarks for computational techniques (e.g., the comparison between MoM, FEM and FD-TD) and experimental techniques (e.g., the wire antenna) and identified particular computational issues (e.g., extremely ill-conditioned matrices), and they have been the cornerstone for generalizations in two and three dimensions. For example, [4] and [9]

solved the problem of wire antennas with arbitrary shapes; [10] and [11] used telegraphist's equations to evaluate transmission lines by using the Green function; [12] proposed the use of semiorthogonal compactly supported spline wavelets to evaluate an infinitely long metallic cylinder illuminated by a TM plane wave; [13] found the unknown current of a linear dipole with MFIE using high-order basis functions; and [14] and [15] solved the scattering for an infinite curved smooth strip considering the TM and TE cases by using the Nystrom method. However, few discussions exist regarding the relationship between the system theory based on the convolution operator and the Fredholm equation in the context of electrodynamics. Notably, [16] defined an effective bandwidth of a scattered field using the bandlimited behavior of the far field. Subsequently, [17] and [18] used this property to define basis functions with better convergence based on the entire domain and quasi-localized bandlimited interpolation functions. Furthermore, [19] used this behavior to simplify the Green function by removing the unexpected spectral components. This approach was supported by the similarity of the problem with a convolutional formulation, which was not very well defined.

The main contributions of this paper are new design paradigms and strategies for solving a Fredholm equation of the first kind, which covers the MoM methodology. For instance, we found that the functions used to determine a linear equation system can be designed as generalized interpolation functions without the assumption of continuity or smoothness, the weighting functions are sampled linear filters with particular specifications, and the new matrix coefficients ( $S_{mn}$ ) may contain information concerning the supradomain ( $x \in \Omega^c$ ). In the same manner, we proved that the generalized interpolation functions can be different from the functions used to approximate the unknown continuous function, and it is possible to reduce the computational cost based on the properties of *linear and invariant systems*.

The remaining sections of the article are organized as follows: in method of sampling section describes the justification and development of the novel approach using the nonideal instantaneous sampling theory. In analysis and evaluation section, several aspects of the matrix approach are discussed, and two examples are numerically evaluated. In conclusions, we present the conclusions of this research. Finally, appendices A and B detail several definitions, theorems and properties needed to make this paper self-contained.

## Method of Sampling

### Convolutional Equivalence

Assume a convolutional integral equation (CIE) with the form  $\exists g(\cdot): \int_a^b K(x, u)g(u)du = f(x)$  with  $a < b$ ,  $\forall x \in \Omega \triangleq [a, b] \subset \mathbb{R}$  and  $K(x, u) = K(x - u)$ . Let  $K \in L^2$  and  $g_\Omega \in L^{1 \wedge 2}$  with the essential bandwidths being  $BW_2^K$  and  $BW_2^{g_\Omega}$  (see definition 8).

Consider the extended equivalent problem  $\exists g_\Omega(\cdot): \int_{-\infty}^{\infty} K(x, u)g(u)du = f^\infty(x) = f_\Omega^\infty(x) + f_{\Omega^c}^\infty(x)$ , with  $f_\Omega^\infty(x) = f_\Omega(x)$  and  $\Omega^c = \mathbb{R} - \Omega$  [8]. From this formulation, the extended function  $f^\infty(x)$  has two components: The first ( $f_\Omega^\infty$ ) is the known function because  $f_\Omega(x) = \{f(x), \forall x \in \Omega \text{ and zero elsewhere}\}$ ; the second ( $f_{\Omega^c}^\infty$ ) is the extended function  $f^\infty(x)$  evaluated in the supradomain ( $x \in \Omega^c$ ), which is a degree of freedom with mathematical sense allowing the hypothesis  $g_\Omega \xrightarrow{K} f^\infty$ . For a major discussion concerning this equivalence, see [8].

The analysis of this new problem can be performed in the original domain ( $x$  –domain) or the Fourier domain ( $v$  –domain) by using

$$K(x) * g_\Omega(x) = f^\infty(x) \quad (1)$$

$$\tilde{K}(v) \cdot \tilde{g}^\Omega(v) = \tilde{f}^\infty(v) \quad (2)$$

where  $f^\infty \in L^2$  with  $BW_2^{f^\infty}$ . The critical bandwidth of this new problem is denoted by  $BW = \min \{BW_2^{f^\infty}, BW_2^{f_{\Omega^c}^\infty}\}$ .

The solution of this problem must be in the  $x$  –domain because the degree of freedom  $f_{\Omega^c}^\infty(x)$  is unknown, and even though this function makes mathematical sense, it is not related to the physics of the original problem.

### Asymptotic Reduction

Let  $x_n \in \{\dots, x_{-1}, x_0, x_1, \dots\}$  be sampling points such that  $\mathcal{S} \triangleq \{x_1, \dots, x_N\} \subseteq \Omega$  and  $\mathcal{S}^c \triangleq \{\dots, x_{-1}, x_0, x_{N+1}, x_{N+2}, \dots\} \not\subseteq \Omega$ . Let  $\Psi(x)$  be a nonideal sampling function defined by

$$\Psi(x) = \sum_{n=-\infty}^{\infty} \hat{g}_\Omega(x_n) p_n(x; \Delta) \quad (3)$$

$$\mathcal{S} \subseteq \Omega, \Lambda, \mathcal{S}^c \not\subseteq \Omega \quad = \quad \sum_{n=1}^N \hat{g}_\Omega(x_n) p_n(x; \Delta) \quad (4)$$

$$= \quad \hat{g}_\Omega(x) + \epsilon_\Delta(x) \quad (5)$$

where  $\hat{g}_\Omega(x_n)$  is an instantaneous approximation of  $g_\Omega(x_n)$ , and  $p_n(x; \Delta)$  is a generalized interpolation function [8].

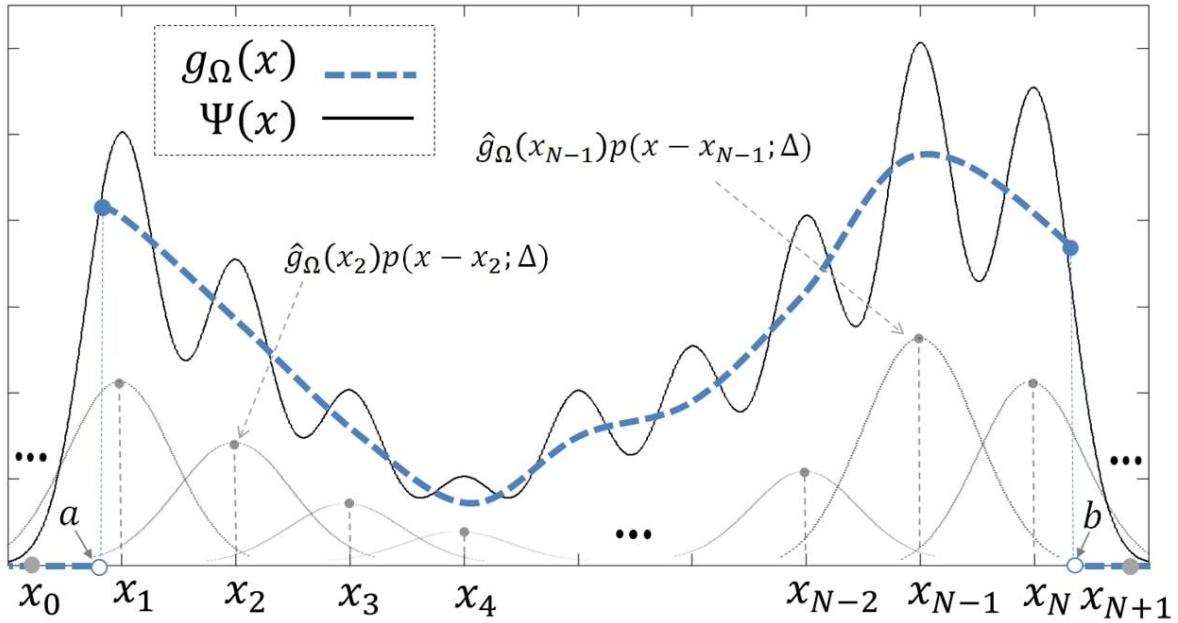
In contrast with other computational methods developed so far, the nonideal sampling function  $\Psi(x)$  is not necessarily a satisfactory representation of  $g_\Omega(x)$  in the conventional sense (e. g., variational sense). This fact means that  $\Psi(x): \Delta > 0$  does not necessarily minimize a continuous error, such as  $\min_{\forall x \in \Omega} \max |\Psi(x) - g_\Omega(x)|$ ,  $\min \int_\Omega |\Psi(x) - g_\Omega(x)| dx$  or  $\min \int_\Omega (\Psi(x) - g_\Omega(x))^2 dx$ , as can be inferred from figure 1. We use functions such that  $\hat{g}_\Omega(x)$  and  $\epsilon_\Delta(x)$  are asymptotically ( $\Delta \rightarrow 0^+$ ) separable through the  $v$ -domain. As a result,  $\Psi(x)$  is not necessarily conformed by a combination of orthogonal or smooth functions with domain  $\Omega$  (see figure 1).

If we use uniform generalized interpolation functions  $p_n(x; \Delta) = p(x - x_n; \Delta) = p(x; \Delta) * \delta(x - x_n)$  with domain  $\Omega_{p_n} \subseteq \mathbb{R}$  and uniform samples  $x_n = x_{n-1} + \Delta = x_0 + n\Delta$ , the spectral error is (see theorem 11)

$$\tilde{\epsilon}_\Delta(v) = \{\Delta^{-1} \cdot \tilde{p}(v; \Delta) - 1\} \cdot \tilde{g}^\Omega(v) + \tilde{\rho}_\Delta(v) \quad (6)$$

$$\tilde{\rho}_\Delta(v) = \Delta^{-1} \cdot \tilde{p}(v; \Delta) \sum_{k=1}^{\infty} \tilde{g}^\Omega(v \pm k\vartheta) e^{\pm 2\pi j \cdot k\vartheta x_0} \quad (7)$$

Figure 1. Conceptual example of a generalized interpolation function proposed in this paper



Source: Páez [8]

Therefore, the spectral error function  $\tilde{\epsilon}_\Delta(v)$  has three spectral components: The first component is the distortion of  $\{\Delta^{-1} \cdot \tilde{p}(v; \Delta) - 1\}$  in  $|v| \leq BW$ . The second component is the interference of  $\tilde{\rho}_\Delta(v)$  in  $|v| > BW$ . From (7), this interference may be centered at the harmonics  $\pm k\vartheta$ , and it may be located in the intervals  $|v \pm k\vartheta| \leq BW$ . The third component is the aliasing of  $\tilde{\rho}_\Delta(v)$  in  $|v| \leq BW$ . Consequently, if

$$\delta_\Delta(x) \triangleq \Delta^{-1} \cdot p(x; \Delta) \quad (8)$$

is a nascent Delta-Dirac function, then the distortion and aliasing are asymptotically removed via  $\tilde{\epsilon}_\Delta(v)$  for  $g_\Omega \in L^{1 \wedge 2}$  using the Nyquist criterion  $\vartheta \triangleq \Delta^{-1} > 2BW$ . If the Nyquist criterion is not satisfied, the aliasing cannot be controlled, and therefore, it is not possible for convergence to occur in the problem.

We assume the new equivalent instantaneous problem in the  $x$ -domain and in the  $v$ -domain to be defined as follows:

$$(K * \Psi)(x) = (K * \hat{g}_\Omega)(x) + (K * \epsilon_\Delta)(x) = f^\infty(x) \quad (9)$$

$$(\tilde{K} \cdot \tilde{\Psi})(v) = (\tilde{K} \cdot \tilde{g}^\Omega)(v) + (\tilde{K} \cdot \tilde{\epsilon}_\Delta)(v) = \tilde{f}^\infty(v) \quad (10)$$

The novel approach is based on the solution of this new problem assuming the *asymptotic reduction* of the spectral error, summarized by

$$\lim_{\Delta \rightarrow 0^+} \|(\tilde{K} \cdot \tilde{\epsilon}_\Delta)(v)\|_2 \rightarrow 0 \quad (11)$$

As a result,  $\hat{g}_\Omega(x) \rightarrow g_\Omega(x)$  and  $\hat{g}_\Omega(x_n) \rightarrow g_\Omega(x_n)$  almost everywhere. Therefore, the relations among the interpolation function  $p(x; \Delta)$ , kernel  $K(x)$  and sampling rate ( $\vartheta \triangleq \Delta^{-1}$ ) to achieve this particular behavior are not arbitrary.

**Remark 1.** Because we do not know  $\hat{g}_\Omega(x)$  *a priori*, our methodology only obtains the instantaneous values  $\hat{g}_\Omega(x_n)$  [8]. Consequently, a smooth interpolation algorithm, denoted by  $\mathcal{I}\{\cdot\}$ , must be used to find the unknown continuous approximation given by  $\hat{g}_\Omega(x) = \mathcal{I}\{\hat{g}_\Omega(x_n)\}$ , under the hypothesis of compliance with the Nyquist criterion.

In contrast with other methodologies, the proposed approach allows the determination of several design strategies and interpretations to solve linear operators using Fourier analysis. For clarity and space reasons, we discuss only two of these strategies below.

### ***Bandwidth Matching Procedure (BM-P)***

We propose a general methodology to solve a CIE assuming that the combination of the interpolation functions and the kernel allows the undervaluing of the influence of the spectral error in the problem, for example, by assuming  $BW_2^{g_\Omega} \gg BW_2^K$  or  $\|(\tilde{K} \cdot \tilde{g}^\Omega)(v)\|_2 \gg \|(\tilde{K} \cdot \tilde{\epsilon}_\Delta)(v)\|_2$ . We name this technique the bandwidth matching procedure (BM-P).

Without loss of generality, if we take samples at  $x = x_m \in \mathcal{S}$  in (9),

$$\sum_{n=1}^N \hat{g}_\Omega(x_n) K(x) * p_n(x; \Delta) \Big|_{x=x_m} = f^\infty(x)|_{x=x_m} \quad (12)$$

Rewriting (12) in integral form, we obtain

$$\sum_{n=1}^N \hat{g}_\Omega(x_n) \int_{-\infty}^{\infty} K(x_m - u) p_n(u; \Delta) du = f(x_m) \quad (13)$$

$$\sum_{n=1}^N \hat{g}_\Omega(x_n) S_{mn} = f(x_m) \quad (14)$$

The linear equation system using BM-P is  $\mathbf{S}\Psi = \mathbf{f}$  with  $\Psi = [\hat{g}_\Omega(x_n)]$ ,  $\mathbf{f} = [f(x_m)]$  and  $\mathbf{S} = [S_{mn}]$ , where  $\hat{g}_\Omega(x_n)$  is an instantaneous approximation of  $g_\Omega(x_n)$ ,  $f(x_m)$  is the instantaneous value printed by the output, and  $S_{mn}$  is the instantaneous equivalent system between the samples, defined as

$$S_{mn} = \int_{-\infty}^{\infty} K(x_m - u) p_n(u; \Delta) du \quad (15)$$

**Corollary 2.** *If we design  $p_n(\cdot; \Delta)$  as the basis functions and  $\Omega_{p_n} \subseteq \Omega$ , the BM-P obtains the same equations as those used by the MoM when using the point matching procedure (PM-P).*

If the Fourier transform of the functions are well-defined and  $\mathcal{F}\{K(x) * p(x; \Delta)\} = \tilde{K}(v) \tilde{p}(v; \Delta)$  holds with  $\tilde{K} \cdot \tilde{p} \in L^1$ , another way to evaluate the system coefficients [8] is by using

$$S_{mn} = \int_{-\infty}^{\infty} \tilde{K}(v) \tilde{p}(v; \Delta) e^{-2\pi j \cdot v(x_n - x_m)} dv \quad (16)$$

### ***Regularization Technique by Convolution (RT)***

We propose another general methodology to solve a CIE assuming some spectral anomaly, for instance  $BW_2^{g_\Omega} \ll BW_2^K$  or  $\|(\tilde{K} \cdot \tilde{g}^\Omega)(v)\|_2 \ll \|(\tilde{K} \cdot \tilde{\epsilon}_\Delta)(v)\|_2$ . In this case, we propose the regulation of (1) using  $R(x; \Delta)$  with the convolution operator (literally, filtering the problem) as

$$R(x; \Delta) * \{K(x) * g_\Omega(x)\} = R(x; \Delta) * f^\infty(x) \triangleq \bar{f}^\infty(x) \quad (17)$$

such that the new system can be modeled as a well-defined low-pass problem with a new critical bandwidth  $\overline{BW} < BW$ . We name this technique as the regularization technique by convolution (RT).

Therefore, to have asymptotic convergence toward the original problem, we design the filter  $R(x; \Delta)$  as a nascent Delta-Dirac function with nulls specifically located to reduce the

spectral anomalies in the problem. In particular, we design these nulls to remove asymptotically the last component of the spectral error, that is, the harmonic interference. Without loss of generality, if we take samples at  $x = x_m \in \mathcal{S}$  in the new equivalent instantaneous problem,

$$\sum_{n=1}^N \hat{g}_\Omega(x_n) R(x; \Delta) * \{K(x) * p_n(x; \Delta)\} \Big|_{x=x_m} = \bar{f}^\infty(x) \Big|_{x=x_m} \quad (18)$$

Rewriting (18) in integral form, we obtain

$$\sum_{n=1}^N \hat{g}_\Omega(x_n) \int_{-\infty}^{\infty} R(x_m - \xi; \Delta) \int_{-\infty}^{\infty} K(\xi - u) p_n(u; \Delta) du d\xi = \int_{-\infty}^{\infty} R(x_m - \xi; \Delta) f^\infty(\xi) d\xi \quad (19)$$

$$\sum_{n=1}^N \hat{g}_\Omega(x_n) \bar{S}_{mn} = \bar{f}^\infty(x_m) \quad (20)$$

where the function  $R_m(\xi; \Delta) = R(x_m - \xi; \Delta)$  is literally the sampled impulse response of a standard linear filter.

The linear equation system using RT is  $\bar{\mathbf{S}}\Psi = \bar{\mathbf{f}}$  with  $\Psi = [\hat{g}_\Omega(x_n)]$ ,  $\bar{\mathbf{f}} = [\bar{f}^\infty(x_m)]$  and  $\bar{\mathbf{S}} = [\bar{S}_{mn}]$ , where  $\hat{g}_\Omega(x_n)$  is an instantaneous approximation of  $g_\Omega(x_n)$  considering the filter  $R(x; \Delta)$ ,  $\bar{f}^\infty(x_m)$  is the instantaneous value printed by the regularized output, and  $\bar{S}_{mn}$  is the new instantaneous equivalent system between the samples given by

$$\bar{S}_{mn} = \int_{-\infty}^{\infty} R_m(\xi; \Delta) \int_{-\infty}^{\infty} K(\xi - u) p_n(u; \Delta) du \quad (21)$$

$$\bar{f}^\infty(x_m) = \int_{-\infty}^{\infty} R_m(\xi; \Delta) f^\infty(\xi) d\xi \quad (22)$$

If we design  $R_m(\xi; \Delta)$  with subdomains ( $\Omega_{R_m} \subset \Omega$ ) or entire domains ( $\Omega_{R_m} = \Omega$ ) to avoid unknown information of  $f^\infty(x)$ , the resulting respective techniques are called the subdomain regularization technique (S-RT) and the entire domain regularization technique (E-RT).

**Corollary 3.** *If we design  $p_n(\cdot; \Delta)$  as the basis functions,  $R_m(\cdot; \Delta)$  as the weighting functions related to an interior product, and  $\Omega_{p_n}, \Omega_{R_m} \subseteq \Omega$ , the RT obtains the same equations as*

those used when applying the general approach of the MoM (and in general, those employed when using the MWR).

If it is possible to use the associativity property  $R * \{K * \Psi\} = \{R * K\} * \Psi = K * \{R * \Psi\}$  (e.g., see Fubini's theorem and Hölder's inequality), the formulation can be simplified and computational cost can be reduced by using  $\sum_{n=1}^N \hat{g}_\Omega(x_n) K(x) * P_n(x; \Delta) = \bar{f}^\infty(x)$  because  $P_n(x; \Delta) \triangleq (R * p_n)(x; \Delta)$  and  $\Omega_{P_n} \triangleq \Omega_R * \Omega_{p_n}$  may have closed forms. The new function  $P_n(x; \Delta)$  is known as an ultrafunction, and the simplified formulation as termed as the ultra-RT. In this case, the system coefficients [8] can be obtained using

$$\bar{S}_{mn} = \int_{-\infty}^{\infty} K(x_m - u) P_n(u; \Delta) du \quad (23)$$

$$= \int_{-\infty}^{\infty} K(x_n - x_m - u) P(u; \Delta) du \quad (24)$$

$$= \int_{-\infty}^{\infty} K(u) P(x_n - x_m - u; \Delta) du \quad (25)$$

Finally, if the Fourier transforms of the functions are well defined and  $\mathcal{F}\{R(x; \Delta) * K(x) * p(x; \Delta)\} = \tilde{R}(v; \Delta) \tilde{K}(v) \tilde{p}(v; \Delta)$  holds with  $\tilde{R} \cdot \tilde{K} \cdot \tilde{p} \in L^1$ ,

$$S_{mn} = \int_{-\infty}^{\infty} \tilde{R}(v; \Delta) \tilde{K}(v) \tilde{p}(v; \Delta) e^{-2\pi j \cdot v(x_n - x_m)} dv \quad (26)$$

From (10) and (17), if we choose  $R(x; \Delta) = \Delta^{-1} \cdot p(x; \Delta)$ , the harmonic interference can be reduced by using a quadratic factor. In the same way, if the related functions are designed as in the MoM, this technique can be considered an alternative explanation of the Galerkin method, and it can easily explain under what conditions the solution can be successfully applied [8].

### ***Design Considerations***

The asymptotic reduction is obtained and justified using the sample theory in the following manner. The distortion is asymptotically removed by choosing the interpolation function as a nascent Delta-Dirac function because  $\lim_{\Delta \rightarrow 0^+} \tilde{\delta}_\Delta(v) \rightarrow 1: \forall |v| \leq BW$ . The interference is reduced by designing the interpolation functions (and the filter) with spectral nulls at the harmonic interference, given by  $|\tilde{\delta}_\Delta(v)| \leq \delta_l \ll 1, \forall |v \pm k\vartheta| \leq BW, k \in \mathbb{N}$ . This interference is asymptotically removed by increasing the sampling rate because the kernel

has a finite bandwidth. The spectral nulls should be designed to exactly match with this interference to reduce the possibility of occurrence of ambiguities caused by the nonexistence of  $f_{\Omega}^{\infty}(x)$ . Finally, the aliasing is asymptotically removed by increasing the sampling rate because  $\forall \hat{g}_{\Omega} \in L^{1\wedge 2}$  has the property  $\lim_{v \rightarrow \infty} \tilde{g}^{\Omega}(v) \rightarrow 0$ . As a result,  $\lim_{\Delta \rightarrow 0^+} \tilde{g}^{\Omega}(v \pm k\vartheta) \rightarrow 0: \forall |v| \leq BW, k \in \mathbb{N}$  and  $\lim_{\Delta \rightarrow 0^+} \tilde{p}_{\Delta}(v) \rightarrow 0: \forall |v| \leq BW$ . For details and examples of these considerations, see [8].

## **Analysis and Evaluation**

### ***Novel Approach to Solve Convolutional Integral Equations***

Because the approach of the MoS! has a different way to obtain convergence, to the best of the author's knowledge, our proposal is an innovative framework for solving Fredholm equations of the first kind. The MWR solves  $\exists g(\cdot): \mathcal{L}\{g\} = f$  by using  $\hat{g} = \sum_{n=1}^N \alpha_n b_n$ , such that the residual error  $r = \mathcal{L}\{\hat{g}\} - f$  is reduced by means of the interior product  $\langle r, R_m \rangle = 0$  [4]. The novel approach includes the same interpretation because the same equations are determined when  $\Omega_{p_n}, \Omega_{R_m} \subseteq \Omega$ , albeit with new paradigms and degrees of freedom. We highlight the following aspects of our methodology.

Before taking the samples  $x_m$  in (12) and (18), the functions  $p(x; \Delta)$  and  $R(x; \Delta)$  can be designed to reduce the error in both domains because  $\|\tilde{\epsilon}_{\Delta}(v)\|_2 = \|\epsilon_{\Delta}(x)\|_2$ . A more comprehensive approach to design  $R(x; \Delta)$  (and the problem) using the *communication theory* may be considered because that function is not necessarily related to a reduction in the residual error in the sense of a geometric projection. For instance, the filter  $R(\cdot; \Delta)$  may be designed as a standard receptor system with several roles related to reducing the noise caused by the rounding errors (e. g., pre-emphasis and de-emphasis techniques and matched filter) and transforming a dense matrix in a sparse matrix (e. g., intersymbol interference techniques).

After taking the samples  $x_m$  in (12) and (18), the obtained matrices  $\mathbf{S}\Psi = \mathbf{f}$  and  $\bar{\mathbf{S}}\Psi = \bar{\mathbf{f}}$  are the formulations of a standard discrete-time system (formally a discrete  $x$ -domain system), in which it is now evident that all the information between the samples  $x_m$  and  $x_{m+1}$  is lost because, in general,  $f^{\infty}(x)$  and  $\bar{f}^{\infty}(x)$  are not bandlimited functions. As a result,  $\Psi(x)$  is not necessarily a good continuous approximation of the unknown function  $g_{\Omega}(x)$ .

**Remark 4.** The only methodological difference between BM-P and RT is that the original problem is regularized by a filter to obtain a slower problem. As a consequence, the MoM (and, in general, the MWR) is an instantaneous technique, or “point matching procedure”, independent of the weighting functions.

### Discussion Concerning Interpolation Functions

A standard interpolation function is defined as a basis function in the context of being used by standard numerical methods such as the MoM. For instance, the well-known rectangular and triangular basis functions are  $p_n^\Pi(x; \Delta) = \Pi_\Delta(x - x_n)$  and  $p_n^\Lambda(x; \Delta) = \Lambda_\Delta(x - x_n)$ . Our approach allows the analysis of these functions because their Fourier transforms are well defined by  $\tilde{p}^\Pi(v; \Delta) = \vartheta^{-1} \text{sinc}(\pi v / \vartheta)$  and  $\tilde{p}^\Lambda(v; \Delta) = \vartheta^{-1} \text{sinc}^2(\pi v / \vartheta)$ .

Consequently, to maintain the distortion in  $0.95 \leq |\Delta^{-1} \cdot \tilde{p}(v; \Delta)| \leq 1, \forall |v| \leq BW$ , it is required that  $BW \leq 0.175\vartheta$  and  $BW \leq 0.124\vartheta$ . As a result, the minimum sampling rate with that distortion for  $p^\Pi(\cdot; \Delta)$  is  $\vartheta = 0.175^{-1}BW \geq 6 \cdot BW$  and that for  $p^\Lambda(\cdot; \Delta)$  is  $\vartheta = 0.124^{-1}BW \geq 9 \cdot BW$ .

These results prove that if the kernel has a narrow bandwidth such that it reduces the interference of the sampling process, the rectangular function should unexpectedly obtain a better accuracy than the triangular function does because the distortion is lower at the same sample rate.

In contrast, because the reduction in the first harmonic interference is given by  $|\Delta^{-1} \cdot \tilde{p}(v; \Delta)| < \delta_f^{\pm 1}, \forall |v \pm \vartheta| < BW$  with  $\delta_f^{\pm 1, \Pi} = 0.2016$  and  $\delta_f^{\pm 1, \Lambda} = 0.0192$ , the triangular function should demonstrate superior performance in the kernels with wide bandwidths (e. g., kernels with some singularity or quasi-singularity) because the main harmonic interference of the sampling process is one decade lower at the same sample rate. From our approach, it is now evident that the rectangular function does not necessarily minimize  $\|\Psi(x) - g_\Omega(x)\|$ , although the instantaneous value  $\hat{g}_\Omega(x_n)$  may be more accurate.

A generalized interpolation function is defined in a different direction using the asymptotic separability in the  $v$  –domain between the unknown approximation and the error. As a result,  $\Psi(x)$  may not be a standard representation of  $g_\Omega(x)$  (see figure 1). Nevertheless, these functions require careful design to avoid the numerical instability caused by the spectral mismatch (e. g., new spectral nulls in the problem). An uncomplicated method to formulate a generalized interpolation function is

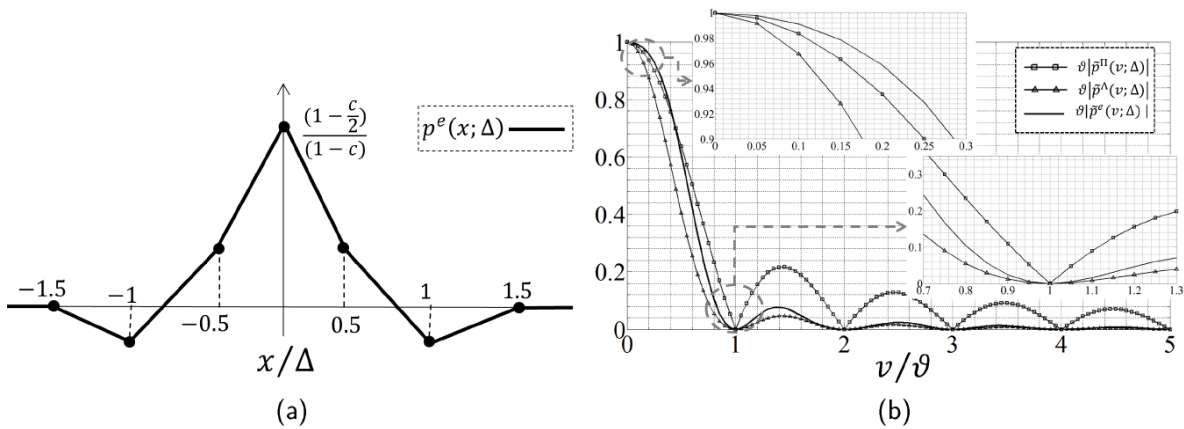
$$p(x; \Delta) = (p^1 * \dots * p^M)(x; \Delta) \triangleq \prod_{i=1}^M p^i(x; \Delta) \quad (27)$$

where  $\tilde{p}(v; \Delta) = \prod_{i=1}^M \tilde{p}^i(v; \Delta)$  and  $\Delta^{-1} \cdot p(x; \Delta)$  represent a nascent Delta-Dirac function with nulls located strictly in the harmonic interference of the sampling process. To demonstrate this methodology, the authors propose  $p^e(x; \Delta) = (p^1 * p^2)(x; \Delta)$  as an example, such that  $p^1(x; \Delta) = \Pi_{\Delta}(x) - \frac{c}{2}\Pi_{\Delta}(x + \frac{\Delta}{2}) - \frac{c}{2}\Pi_{\Delta}(x - \frac{\Delta}{2})$  and  $p^2(x; \Delta) = t_1 \cdot \Pi_{\Delta}(x)$ , as shown in figure 2a.

**Figure 2. Generalized interpolation function  $p^e(x; \Delta)$**

**(a) Model in the  $(x/\Delta)$  –domain**

**(b) Model in the  $(v/\vartheta)$  –domain**



Source: Páez [8]

The formulation of this unusual combination in the  $v$  –domain is  $\tilde{p}^e(v; \Delta) = (\tilde{p}^1 \cdot \tilde{p}^2)(v; \Delta) = t_1 \vartheta^{-2} \text{sinc}^2(\pi v/\vartheta) \{1 - c \cdot \cos(\pi v/\vartheta)\}$ ; therefore, to achieve the nascent Delta-Dirac behavior, the constant  $t_1 = \vartheta/(1 - c)$ . Figure 2b shows that if  $c = 1/3$ ,  $\tilde{p}^e(v; \Delta)$  increases the linearity regarding  $\tilde{p}^1(v; \Delta)$ , and the spectral nulls have a similar attenuation to  $\tilde{p}^1(v; \Delta)$ . As a result, using low-pass kernels, this interpolation function ought to exhibit better performance and low computational cost. The function defined in this example is similar to those defined by the wavelet theory, although it does not necessarily imply a good continuous representation of the original function or a multiresolution signal decomposition.

**Remark 5.** Because the rectangular and triangular functions are nascent Delta-Dirac functions with nulls at  $\pm k\vartheta$ , that basis functions are generalized interpolation functions, as well. The main difference between MoM and MoS! in these cases it is that the instantaneous values  $\hat{g}_{\Omega}(x_n)$  may allow a better continuous approximation than  $\Psi(x)$  does. Finally, if  $|\tilde{K}(v)|$  is strongly decreasing toward zero at high frequencies, it is possible to define

$$p^\delta(x; \Delta) = \Delta \cdot \delta(x) \quad (28)$$

because (46) is proved from (45). As a result, some low-pass kernels may have a convergent closed-form matrix using high sampling rates ( $\vartheta \uparrow$ ), which allows the study of an analytic or asymptotic inverse for the problem, using the digital signal processing framework.

### **Example 1: A Narrow Band Kernel**

The problem  $\int_0^1 |x - u|g(u)du = f(x)$  with  $\forall x, u \in [0,1]$  is the CIE of the differential equation  $g(x) = \frac{1}{2} \frac{d^2}{dx^2} f(x), \forall x \in [0,1]$ , where  $f(x)$  is not an arbitrary function. This function must have some properties [1] such as appropriate boundaries  $f(0)$  and  $f(1)$ , and it must be a bounded twice-differentiable function with a bounded first derivative. As a theoretical and numerical benchmark, we propose  $f(x) = \pi^{-1} - 2\pi^{-2} \sin(\pi x), \forall x \in [0,1]$  and  $g(x) = \sin(\pi x), \forall x \in [0,1]$

Using our approach, the extended convolutional model is

$$|x| * g_\Omega(x) = f^\infty(x) \quad (29)$$

where  $\Omega = [0,1]$ ,  $K(x) = |x|$ ,  $f_\Omega^\infty(x) = f_\Omega(x)$ , and  $f_\Omega^{\infty c}(x)$  is a degree of freedom with mathematical sense. Because  $\frac{d}{dx} |x| = \text{sgn}(x), \forall x \neq 0, \tilde{K}(v) = -\frac{1}{2\pi^2 v^2}, \forall v \neq 0$ .

In this problem, it not possible to use the  $v$ -domain to calculate the matrix coefficients because  $\tilde{K}(v)$  has a distribution not calculated at  $v = 0$ . However, the Fourier domain interpretation is reasonably valid because the Fourier transform is well defined using the distribution theory, and the convolution operator is well established in this problem for a finite interval  $\Omega$ . As a result, by using the spectral interpretation for  $\forall v \neq 0$ , it is valid to assume that this problem is a narrowband kernel for  $BW \geq \pi^{-1}2^{-1/2}$ .

The matrix formulation simplifying  $\Omega = (0,1)$  for  $p^\Pi(x; \Delta)$  is  $(\mathbf{I} + 4\mathbf{B})\Psi = 4\vartheta^2 \mathbf{f}$ , where  $\mathbf{B} = [B_{mn}] = [|m - n|]$  and  $\mathbf{I}$  is the identity matrix; for  $p^\Lambda(x; \Delta)$  is  $(\mathbf{I} + 3\mathbf{B})\Psi = 3\vartheta^2 \mathbf{f}$ , and for  $p^\Pi(x; \Delta)$  and  $R^\Pi(x; \Delta) = \Delta^{-1}\Pi_\Delta(x)$  is  $(\mathbf{I} + 3\mathbf{B})\Psi = 3\vartheta^2 \bar{\mathbf{f}}$ , where  $\bar{f}_m = \pi^{-1} - 2\pi^{-2} \sin(\pi x_m) \text{sinc}(\frac{1}{2}\pi\Delta)$ . From the MoM approach, the first two formulations pertain to the PM-P, and the last one pertains to the Galerkin method.

The matrix formulation using the MoS!-1D with  $p^e(x; \Delta)$  is  $(\mathbf{T} + \mathbf{B})\Psi = \vartheta^2 \mathbf{f}$ , where  $\mathbf{T}$  is an uniform tridiagonal matrix with coefficients  $T_{1,1} = 12^{-1}(4 - 7c)(1 - c)^{-1}$  and  $T_{1,2} = 24^{-1}(24 - 25c)(1 - c)^{-1} - 1$ . We emphasize that this solution is different from the MoM approach because the integrals have different domains.

Figure 3 compares the different estimations through the relative residual error

$$\|\hat{g}_\Theta(x_n) - g_\Theta(x_n)\|_2 / \|g_\Omega(x_n)\|_2 \quad (30)$$

for  $\Theta \triangleq [10, 1 - 10\Delta]$ ; in this case, several new paradigms are evident. Because a low-pass kernel is more relevant for the distortion rather than the interference, the function  $p^\Pi(\cdot)$  finds a better outcome than  $p^\Lambda(\cdot)$  does, and the new proposal  $p^e(\cdot)$  has a significantly better performance for  $\Theta$ , with a different slope (logarithm) of convergence. For instance, the number of unknown variables for an instantaneous relative residual error of  $10^{-7}$  is  $N \approx 50$  for  $p^e(\cdot)$  using the MoS! and  $N \approx 2000$  for the classical low order functions using the MoM.

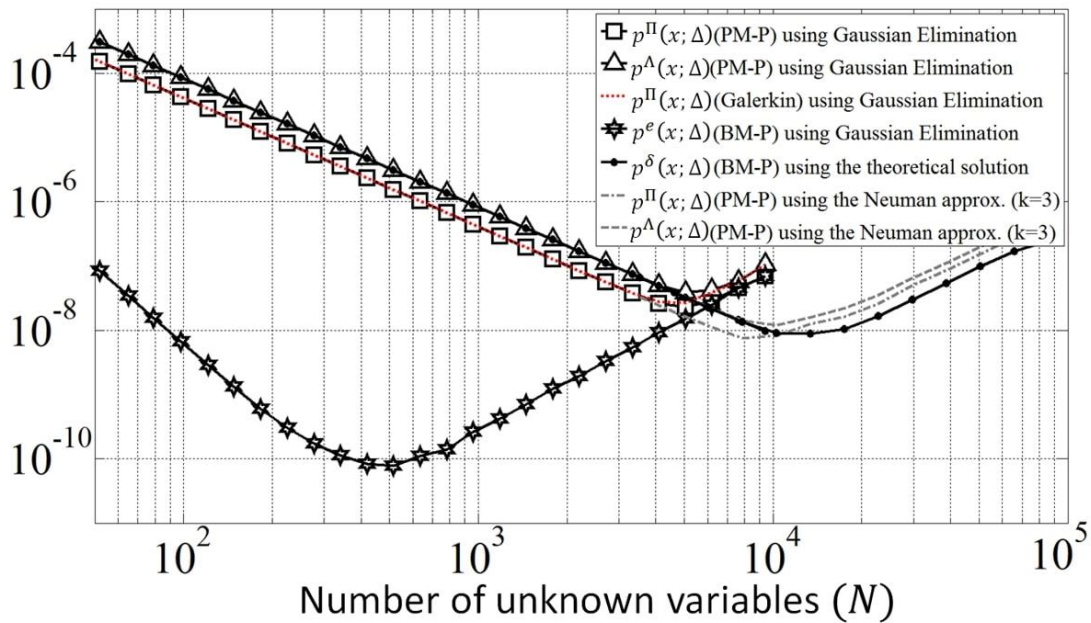
Nevertheless, we note that  $p^\Lambda(\cdot)$  still exhibits better elimination of the first harmonic interference in figure 2b. This little energy is accumulated at the boundaries at  $x_n \in (0, 9\Delta] \cup [1 - 9\Delta, 1)$ . As a result, this location is the only one at which  $p^\Lambda(\cdot)$  exhibits better performance in this problem.

Considering special interpolation functions, we found an inverse with linear complexity using  $p^\delta(x; \Delta)$ . The solution in this case is  $\Psi = \Delta^{-2} \mathbf{B}^{-1} \mathbf{f}$ , where  $\mathbf{B}^{-1}$  is detailed in appendix B. This matrix solution is similar to the matrix used by FDM for  $g(x) = \frac{1}{2} \frac{d^2}{dx^2} f(x)$ . This solution exhibits the same performance as  $p^\Lambda(\cdot)$ , thereby proving conclusively that the interference is not dominant in this problem. The theoretical matrix  $\mathbf{B}^{-1}$  allows the solution of the general case  $(\mathbf{I} + \beta \mathbf{B})\Psi = \beta \vartheta^2 \mathbf{f}$  by applying the *Neuman series* by means of  $\Psi \approx \{\beta^{-1} \mathbf{B}^{-1} + \dots + (-1)^{k+1} \beta^{-k} \mathbf{B}^{-k}\} \beta \vartheta^2 \mathbf{f}$  for  $N \geq 3$  and  $\rho^+(\beta^{-1} \mathbf{B}^{-1}) < 2\beta^{-1} < 1$ . As shown in figure 3, this algorithm converges with  $k = 3$  in the same way as Gaussian elimination for the rectangular ( $\beta = 4$ ) and triangular ( $\beta = 3$ ) cases.

This problem exhibits ill conditioning at high sampling rates (or breakdown segmentation) because this kernel has extremely low spectral information at extremely high frequencies. From figure 3, the breakdown for the classical basis functions can be noted at  $N \gtrsim 4000$  and that for  $p^e(\cdot)$  can be noted at  $N \gtrsim 400$ .

In summary, several of the new paradigms were distinguished in this example. First, we demonstrated that  $\Psi(x)$  is not necessarily the best way to represent the unknown function because the rectangular function exhibits a better instantaneous performance than the triangular function does. Second, we demonstrated that the Galerkin method does not increase the accuracy because this problem is not anomalous at high frequencies. Consistent with the ultraformulation, the same system matrix is found using the triangular function with PM-P and the rectangular function with the Galerkin method. As a consequence, any difference between both results can only be interpreted by filtering of the source. Third, considering the example of  $p^e(x; \Delta)$ , the use of generalized interpolation functions with supradomain information can significantly increase the accuracy. Finally, we demonstrated that the formulation based on  $p^\delta(x; \Delta)$  can be used to design asymptotic techniques to solve this narrowband problem.

Figure 3. Instantaneous relative residual error using different interpolation functions in example 1



Source: Páez [8]

### Example 2: A Wideband Kernel

To discuss the novel approach using a standard electromagnetic benchmark, the authors solved the unknown current of a linear dipole with radio  $0 < a \leq 10^{-2}\lambda$  and length  $L \gg a$  using the reduced or approximate Pocklington equation under a particular printed source  $E(x)$ . Without loss of generality, we use the Richmond simplification [20] to use a standard CIE. The extended convolutional problem is

$$E^\infty(x) = K_{ap}(x) * I_\Omega(x) \quad (31)$$

$$K_{ap}(x) = K_0 G_{ap}(r) r^{-4} (k^2 a^2 r^2 + (1 + jkr)(2r^2 - 3a^2)) \quad (32)$$

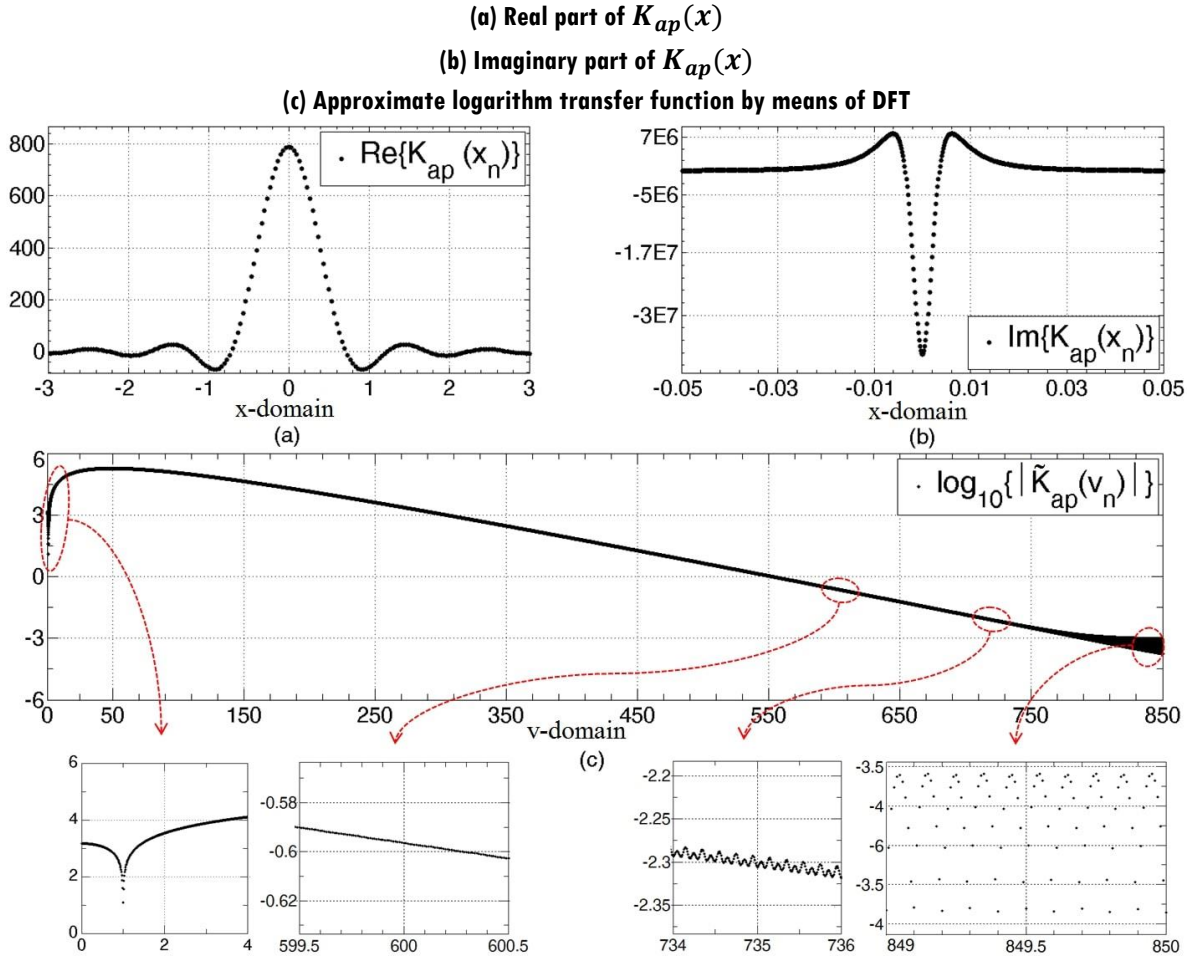
$$G_{ap}(r) = \frac{e^{-jkr}}{4\pi r} \quad (33)$$

$$r = \sqrt{x^2 + a^2} \quad (34)$$

where  $x \in \mathbb{R}$ ,  $\Omega = (-\frac{L}{2}, \frac{L}{2})$ ,  $K_0 = j \cdot (2\pi f \epsilon)^{-1}$ ,  $j = \sqrt{-1}$ ,  $c = \lambda f$ ,  $k = 2\pi/\lambda$ ,  $f$  [Hz] is the frequency,  $c$  [m/s] is the speed and  $\lambda$  [m] is the wavelength in a medium with permittivity  $\epsilon$  [F/m],  $E_\Omega^\infty(x) = E_\Omega(x)$  is the printed source in  $\Omega$ , and  $E_{\Omega^c}^\infty(x)$  is a degree of freedom with mathematical sense.

This quasi-singular kernel can be understood from the Fourier transform  $\tilde{K}_{ap}(v) = \mathcal{F}\{K_{ap}(x)\}$  approximated through the DFT with samples  $x_n = \frac{a}{150}n$ . For instance, figure 4c details  $\log_{10}|\tilde{K}_{ap}(v_n)|$  using  $a = 0.05\lambda$  and  $\lambda = 1$  m, in which several behaviors are evident.

Figure 4. Reduced kernel using  $\alpha = 0.005\lambda$  and  $\lambda = 1$



Source: Páez [8]

As expected, this kernel has a large bandwidth caused by its quasi-singularity. We find a local minimum at  $v = \pm 1$  (and, in general, at  $v = \pm\lambda^{-1}$ ) related to the main spatial harmonic of the unknown current, and a local maximum at  $v \approx \pm 50$  (and, in general, at  $v = \pm \frac{1}{4}a^{-1}$ ). Moreover, the transfer function has an exponential decay for  $|v| \gtrsim 200$ , whose value tends rapidly toward zero. Although the bounded oscillations in  $|v| \gtrsim 600$  have a pseudorandom appearance, they are caused by an infinite  $x$  –domain function with a fast decay toward zero at high frequencies, which is approximated by a truncated function.

To compare the MoM and MoS!, we find the input impedance ( $Z_{in}$ ) of a center-fed dipole using the magnetic frill source simplified by

$$E(x) = \frac{V_s}{2\ln(b/a)} \left\{ \frac{e^{-jk\sqrt{x^2+a^2}}}{\sqrt{x^2+a^2}} - \frac{e^{-jk\sqrt{x^2+b^2}}}{\sqrt{x^2+b^2}} \right\} \quad (35)$$

for all  $x \in \Omega$ ,  $b = 2.3a$  and  $V_S = 1$ . Because the complex power provided by the source is  $S = \frac{1}{2} \int_{-L/2}^{L/2} E(x)I^*(x)dx$ , and it can also be defined using  $S = \frac{1}{2} |I(0)|^2 Z_{in}$ , we estimate the input impedance with the MoM using  $I_\Omega(x) \sim \Psi(x)$  as

$$Z_{in} \approx |\hat{I}_\Omega(0)|^{-2} \int_{-L/2}^{L/2} E(x)\Psi^*(x)dx \quad (36)$$

$$= |\hat{I}_\Omega(0)|^{-2} \sum_{n=1}^N \hat{I}_\Omega^*(x_n) \int_{-L/2}^{L/2} E(x)p_n(x; \Delta)dx \quad (37)$$

In the MoS!, any continuous operation with the unknown current requires the definition of an interpolator because  $\Psi(x)$  loses information between discrete samples. Without loss of generality, we find  $\hat{I}_\Omega(x)$  through the piecewise cubic Hermite interpolating polynomials [21] using  $\hat{I}_\Omega(x_n)$  and the boundaries  $\hat{I}(\pm \frac{L}{2}) = 0$ . Consequently, we estimate the input impedance with the MoS! by using

$$Z_{in} \approx |\hat{I}_\Omega(0)|^{-2} \int_{-L/2}^{L/2} E(x)\hat{I}_\Omega^*(x)dx \quad (38)$$

Furthermore, the difference between the MoS! and MoM is particularly accentuated when we use bandlimited interpolation functions. For instance, and only to differentiate between the methods, if  $p(x; \Delta) = \text{sinc}(\pi x \Delta^{-1})$  with  $x_n = -L/2 + \Delta \cdot n$  and  $\Delta = L/(N + 1)$ , PM-P obtains an impedance matrix ( $\mathbf{Z}$ ) with coefficients

$$Z_{mn} = \int_{-L/2}^{L/2} K_{ap}(x_m - u)\text{sinc}(\pi(u - x_n)\Delta^{-1})du \quad (39)$$

Therefore,  $O(N^2)$  is required to ensure computational storage and  $O(N^3)$  is required to solve the linear equation system using Gaussian elimination because the impedance matrix does not have useful properties. In contrast, the system matrix ( $\mathbf{S}$ ) obtained by (15) is a symmetric Toeplitz matrix, which only requires  $O(N)$  for computational storage, and several efficient algorithms are available to solve the linear equation system [22]. We compare  $Z_{in}$  using PM-P and BM-P with  $L = 0.47\lambda$  in table 1a.

Another application of the MoS! is to use the system matrix as a preconditioner for the MoM because  $\mathbf{S}^{-1}\mathbf{E}$  may lead to a low computational cost and both formulations are closely related at  $x_m, x_n \in \mathcal{S}$ . As an example, figure 5 shows the relative residual error in solving  $\mathbf{Z}\Psi = \mathbf{E}$  using  $\text{sinc}(\cdot)$  and the *conjugate gradient squared method* (CGS) with and

without the preconditioner  $\mathbf{S}$ . As shown, the solution with the preconditioner  $\mathbf{S}$  has fast convergence, even for a small number of unknown variables ( $N$ ).

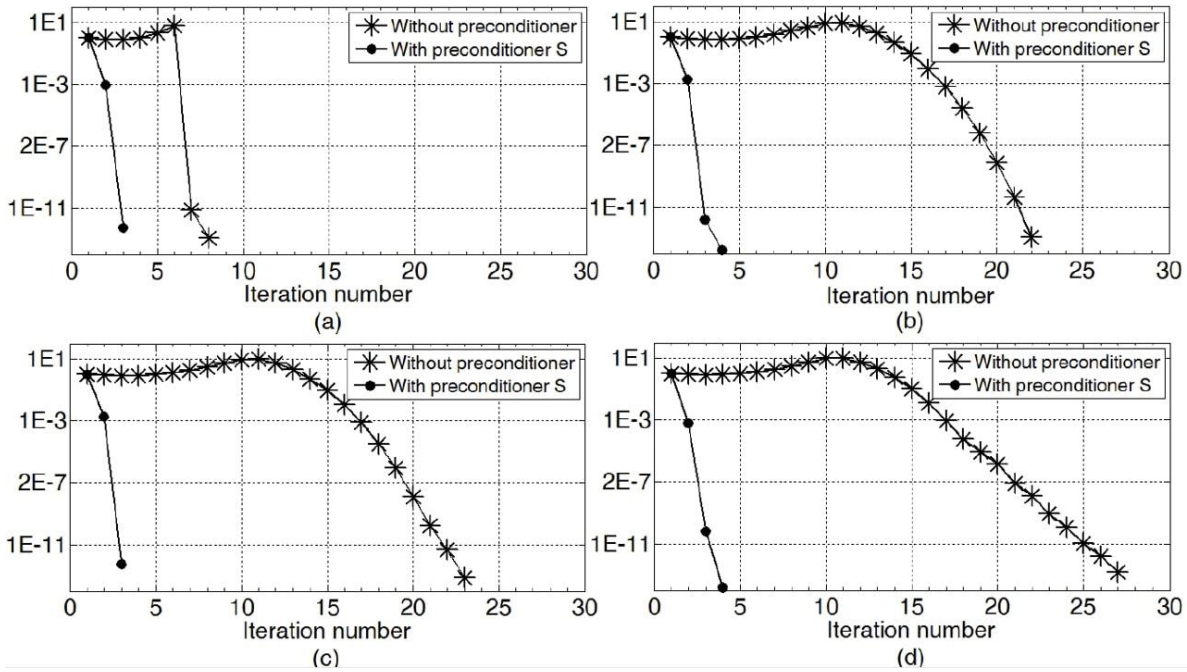
**Figure 5. Relative residual error at  $Z_{N \times N} \Psi = E$  with CGS**

(a)  $N = 11$

(b)  $N = 53$

(c)  $N = 95$

(d)  $N = 137$



Source: Páez [8]

Although the unknown current has a well-identified fundamental harmonic at  $v = \pm 1$ , a considerable bandwidth ( $BW > \frac{1}{2\Delta} \Big|_{N=101} = \frac{N+1}{2L} \Big|_{N=101} = 108.5$ ) is necessary to obtain an absolute relative error less than 3.5% in the imaginary part. The analysis of the magnetic frill source shows that its bandwidth is the cause of this situation. If we assume that  $Z_{in}$  is mainly obtained from band base information, filtering the source with the normalized filter  $R^\Lambda(x; \Delta) = \Delta^{-1} \Lambda_\Delta(x)$  should increase the convergence rate, as shown in table 1b.

**Table 1. Input impedance ( $Z_{in}$ ) for a center-fed dipole using the  $\text{sinc}(\cdot)$  interpolation function with  $L = 0,47\lambda$  and  $\alpha = 0,005\lambda$**

**(a) Basic approach with PM-P and BM-P**  
**(b) Subdomain regularization technique with MoM and S-RT**  
**(c) Galerkin method (MoM)**

N	(a)		(b)		(c)
	PM-P	BM-P	MoM	S-RT	
5	11.52 - 5.48i	11.32 - 5.93i	68.65 - 1.33i	66.23 - 8.46i	66.08 - 5.73i
11	24.95 - 3.94i	24.67 - 4.49i	73.26 + 3.26i	71.20 - 0.81i	73.13 + 0.176i
17	37.58 - 2.05i	37.29 - 2.71i	74.13 + 5.71i	72.88 + 2.68i	72.51 + 3.71i
23	48.38 - 0.01i	48.01 - 0.74i	75.19 + 7.26i	73.99 + 4.82i	75.00 + 5.72i
29	56.81 + 1.20i	56.45 + 1.20i	75.61 + 8.43i	74.69 + 6.34i	74.56 + 7.22i
35	63.08 + 3.80i	62.66 + 2.98i	76.17 + 9.34i	75.28 + 7.51i	76.10 + 8.41i
41	67.46 + 5.37i	67.07 + 4.52i	76.46 + 10.10i	75.71 + 8.44i	75.70 + 9.29i
47	70.55 + 6.69i	70.12 + 5.84i	76.84 + 10.74i	76.11 + 9.22i	76.87 + 10.14i
53	72.63 + 7.81i	72.23 + 6.94i	77.06 + 11.30i	76.41 + 9.89i	76.46 + 10.74i
59	74.11 + 8.74i	73.69 + 7.88i	77.34 + 11.79i	76.71 + 10.47i	77.45 + 11.40i
65	75.12 + 9.53i	74.72 + 8.68i	77.53 + 12.23i	76.95 + 10.98i	77.03 + 11.83i
71	75.88 + 10.21i	75.47 + 9.37i	77.75 + 12.63i	77.18 + 11.44i	77.91 + 12.38i

Source: Páez [8]

We compare the results with those obtained using the Galerkin method in table 1c. According to our approach, the Galerkin method obtains an oscillatory convergence rate because filters conformed by truncated sinc functions do not have well located spectral nulls to ensure the efficient elimination of the interference.

The  $Z_{in}$  evaluated using the ultraformulation (23)-(25) and using the  $v$  -domain (16), (26) exhibit relative residual errors that are less than  $1 \times 10^{-5}$ . In particular, using the symmetric of (32), we simplify (16) and (26) using  $R^\Lambda(\cdot)$  by using

$$S_{mn} = 2\Delta \int_0^{2^{-1}\Delta^{-1}} \cos(2\pi(m-n)v\Delta) \cdot \tilde{K}_{ap}(v)dv \quad (40)$$

$$\bar{S}_{mn} = 2\Delta \int_0^{2^{-1}\Delta^{-1}} \cos(2\pi(m-n)v\Delta) \cdot \text{sinc}^2(\pi v\Delta) \cdot \tilde{K}_{ap}(v)dv \quad (41)$$

Although (40)-(41) have some disadvantages caused by the Fourier transform estimation and the evaluation of an integrand with an oscillatory behavior, they have other advantages

owing to the prior theoretical knowledge of  $\tilde{R}(\cdot)$  and  $\tilde{p}(\cdot)$ , the finite interval of integration, the use of the FFT for a fast calculation and windowing to reduce the truncation effect over  $\tilde{K}_{ap}(v)$ . The system coefficients calculated by  $v$  –domain are a relevant option for other more convenient bandlimited interpolation functions, such as the raised cosine functions.

In conclusion, using potentially the most critical bandlimited interpolation function, we demonstrate that the MoS! is a viable alternative with low computational cost because the new matrix has useful properties based on symmetry, and it can be calculated using low cost alternative expressions. Although the MoM has a better convergence rate in this example, the solution of  $\bar{\mathbf{S}}_{N+18}$  is mostly equivalent to  $\bar{\mathbf{Z}}_N$ . Moreover, we show that the system matrix can be used as a preconditioner for the MoM using a well-known Krylov subspace iterative method with very fast convergence.

Furthermore, the MoS! can simplify the solution using subdomain functions because the ultraformulation is well defined for  $K \in L^2$ . For such a case, we emphasize that if  $\Omega_{p_n}, \Omega_{R_m} \subseteq \Omega$ , both matrices are equal ( $\mathbf{S} = \mathbf{Z}$ ). However, the input impedance is different because both methods employ different approaches for the unknown continuous approximation. In this example, this difference is smaller because the input impedance is calculated using an integral operator (a low-pass operator). To discuss the ultraformulation, we first evaluated  $Z_{in}$  in tables 2a and b using the rectangular and triangular functions with PM-P (and BM-P in the parenthesis) using (15), and MoM (and S-RT in the parenthesis) with the filter  $R^\Lambda(\cdot)$  using (21). As expected, the rectangular function with BM-P exhibited an oscillatory behavior without convergence because the reduced kernel has low attenuation for its interference (see figure 4c in  $|v| \leq 50$ ).

Because  $(R^\Lambda * p^\Pi)(x; \Delta)$  and  $(R^\Lambda * p^\Lambda)(x; \Delta)$  have closed forms, the ultraformulation has two advantages. The first advantage is the reduction of the computational cost owing to the transformation of the 2D integral to 1D. The second advantage is the reduction of the nontrivial effects of rounding errors. In particular, (24) reduces the jitter produced between the interpolation functions and filters, and (25) reduces the jitter produced by the kernel. For instance, we note that the input impedance in table 2b using  $p^\Pi(\cdot)$  and  $R^\Lambda(\cdot)$  must lead to better performance because the kernel and the source have been filtered. Table 2c summarizes the new estimation using (24), in which we remove the lack of convergence without changing the numerical methods. We highlight this nontrivial issue because  $\kappa(\bar{\mathbf{S}}_N) \leq 600$  for  $N \leq 113$ .

**Table 2. Input impedance ( $Z_{in}$ ) for a center-fed dipole using classical subdomain functions with  $L = 0,47\lambda$  and  $a = 0,005\lambda$**

**(a) Basic approach with PM-P (and BM-P)**

**(b) Subdomain regularization technique with MoM (and RT)**

**(c) Ultraformulation using (24)**

**(d) Entire domain regularization technique with MoM (and RT)**

N	(a) PM-P (and BM-P)		(b) MoM (and RT): $R^\Lambda(x; \Delta)$		(c) Ultraformulation $(p^\Pi * R^\Lambda)(x; \Delta)$ using (37) (and (38))	(d) MoM (and RT): $R_\Omega^g(x; \Delta)$	
	$p^\Pi(x; \Delta)$	$p^\Lambda(x; \Delta)$	$p^\Pi(x; \Delta)$	$p^\Lambda(x; \Delta)$		$p^\Pi(x; \Delta)$	$p^\Lambda(x; \Delta)$
5	14.02 + 7.76i (14.00 + 7.79i)	8.63 - 80.24i (8.69 - 81.59i)	65.98 - 10.34i (65.89 - 10.21i)	68.56 + 0.49i (69.07 + 0.19i)	66.02 - 10.21i (65.93 - 10.08i)	73.82 + 10.95i (73.72 + 11.07i)	74.90 + 16.29i (75.50 + 16.04i)
11	25.36 - 3.06i (25.34 - 3.00i)	19.70 - 59.00i (19.75 - 59.56i)	71.13 - 0.9i (71.10 - 0.76i)	73.39 + 5.45i (73.60 + 5.11i)	71.13 - 0.90i (71.10 - 0.76i)	75.04 + 8.36i (75.01 + 8.52i)	76.52 + 12.52i (76.73 + 12.18i)
17	36.97 - 5.19i (36.96 - 5.13i)	31.83 - 41.77i (31.87 - 42.05i)	72.71 + 1.18i (72.71 + 1.30i)	74.85 + 7.38i (74.96 + 7.07i)	72.98 + 2.84i (72.98 + 2.96i)	75.53 + 8.53i (75.52 + 8.66i)	76.85 + 11.89i (76.96 + 11.57i)
23	44.82 - 18.18i (44.82 - 18.13i)	43.30 - 27.72i (43.34 - 27.89i)	74.12 + 5.07i (74.12 + 5.15i)	75.64 + 8.62i (75.70 + 8.35i)	74.06 + 5.10i (74.06 + 5.18i)	75.95 + 9.14i (75.95 + 9.22i)	77.12 + 11.91i (77.19 + 11.64i)
29	52.51 - 18.69i (52.51 - 18.66i)	52.91 - 16.70i (52.94 - 16.86i)	74.86 + 6.52i (74.87 + 6.57i)	76.17 + 9.54i (76.22 + 9.31i)	75.08 + 6.81i (75.09 + 6.86i)	76.32 + 9.81i (76.32 + 9.86i)	77.35 + 12.13i (77.40 + 11.89i)
35	61.78 + 1.47i (61.78 + 1.48i)	60.28 - 8.48i (60.30 - 8.62i)	74.34 + 2.35i (74.35 + 2.37i)	76.56 + 10.26i (76.61 + 10.06i)	75.35 + 7.91i (75.36 + 7.93i)	76.63 + 10.40i (76.64 + 10.42i)	77.56 + 12.41i (77.59 + 12.21i)
41	67.92 + 12.30i (67.93 + 12.31i)	65.61 - 2.52i (65.63 - 2.66i)	73.78 - 1.54i (73.79 - 1.54i)	76.90 + 10.87i (76.93 + 10.70i)	75.79 + 8.87i (75.79 + 8.87i)	76.91 + 10.95i (76.917 + 10.96i)	77.74 + 12.70i (77.77 + 12.53i)
47	72.03 + 18.48i (72.04 + 18.48i)	69.34 + 1.71i (69.36 + 1.59i)	72.92 - 6.59i (72.93 - 6.60i)	77.18 + 11.39i (77.19 + 11.24i)	76.14 + 9.66i (76.15 + 9.66i)	77.16 + 11.45i (77.17 + 11.44i)	77.91 + 12.99i (77.93 + 12.84i)
53	71.38 + 5.10i (71.39 + 5.09i)	71.93 + 4.73i (71.94 + 4.61i)	74.62 + 0.79i (74.63 + 0.78i)	77.41 + 11.85i (77.43 + 11.73i)	76.64 + 10.38i (76.64 + 10.36i)	77.38 + 11.89i (77.38 + 11.88i)	78.07 + 13.27i (78.09 + 13.14i)
59	71.75 + 0.18i (71.75 + 0.17i)	73.71 + 6.90i (73.72 + 6.80i)	76.95 + 10.96i (76.96 + 10.94i)	77.63 + 12.31i (77.65 + 12.19i)	76.95 + 10.96i (76.96 + 10.94i)	77.58 + 12.29i (77.59 + 12.28i)	78.22 + 13.54i (78.23 + 13.43i)
65	73.41 + 3.71i (73.41 + 3.69i)	74.94 + 8.45i (74.95 + 8.35i)	73.55 - 5.46i (73.55 - 5.48i)	77.81 + 12.61i (77.82 + 12.52i)	76.97 + 11.43i (76.97 + 11.40i)	77.77 + 12.67i (77.78 + 12.65i)	78.35 + 13.80i (78.36 + 13.70i)
71	71.82 - 7.16i (71.82 - 7.19i)	75.82 + 9.61i (75.82 + 9.53i)	67.60 - 34.30i (67.61 - 34.32i)	77.97 + 12.93i (77.98 + 12.85i)	77.09 + 11.86i (77.09 + 11.84i)	77.94 + 13.02i (77.95 + 12.99i)	78.47 + 14.04i (78.48 + 13.95i)

Source: Páez [8]

Continuing the discussion on regularization, we note that filters with subdomains are inefficient in reducing the source's bandwidth due to the time-frequency relationship (formally, the relationship between the  $x$  and  $v$  domains). To enhance the convergence, we propose the sampled filter  $R_\Omega^g(x_m - x)$  inspired by the standard Gaussian filter

$$R^g(x) = \sigma^{-1} e^{-\pi x^2 / \sigma^2}, \forall x \in \mathbb{R} \quad (42)$$

where  $\sigma = c \cdot \Delta$  to obtain a nascent Delta-Dirac function ( $c \geq 1$ ).

Table 2d shows the recalculation of  $Z_{in}$  using the entire domain filter with  $c = 1.5$ . As shown, it is possible to improve the convergence significantly, even for low order interpolation functions (e. g., tables 1 and 2 show that the triangular interpolation function

with the quasi-Gaussian filter using  $N = 17$  has the same approximate performance as that of the triangular filter using  $N = 41$ , without filter using  $N = 77$ , and with the entire domain formulations using the sinc function and  $N > 53$ ). Nevertheless, some disadvantages were observed when filters were used in this problem. First, the conditioning number and the fake oscillations [23] and [24] may be increased because the filters reduce the bandwidth artificially. Second, the use of any filter includes the establishment of a particular model for the discontinuities at low sampling rates, which implies that a specific model may be used for the current at the feed point and the edges of the wire. Lastly, monotone convergence using the quasi-Gaussian filter when  $c \gtrsim 1.5$  does not occur because spectral mismatches exist in this particular problem (e.g., a relevant transience exists for  $N < 17$  and  $c = 1.5$ ).

In summary, we solved a classical electromagnetic problem with several new paradigms. It was noted that the limiting factor for fast convergence is the bandwidth of the printed source. Therefore, the regularization filter, and not the interpolation function, is the design challenge for a fast and numerically stable solution. Moreover, it was demonstrated that the instantaneous values obtained from the system matrix allow the solution of the problem, and less notably,  $\Psi(x)$  was considered to be an interpolator with an unnecessary high computational cost. According to our approach, the use of  $\Psi(x)$  to calculate other performance parameters based on wideband operators (e.g., vector operators) is not desirable because  $\Psi(x)$  may possess information that is not valid at high frequencies. In particular, the information obtained using the reduced kernel at high frequencies by employing any method is strictly incorrect because the real part of this kernel is an almost ideal low-pass filter with essential bandwidth  $BW_2^{Re\{K_{ap}\}} \approx \lambda^{-1}$ . For these reasons, we changed the terminology of “basis functions” to “interpolation functions” because these functions do not necessarily provide basis for the unknown function following the standard algebraic approach.

## **Conclusions**

The authors presented a novel approach to solve integral equations with difference kernels, based on the generalization of a Fredholm equation of the first kind, as an extended convolutional problem. The results demonstrated that the method of moments (and in general, the method of weighted residuals) is a particular case, in which new interpretations, degrees of freedoms and design rules can be found using standard matrix techniques.

The new approach can be used to address major methodological questions for the method of moments; these questions include those pertaining to the design of all the functions related with the computational method (e.g., to the best of the author’s knowledge, a

general approach for the design of weighting functions has not been reported so far), the establishment of preconditioners in a systematic manner (e.g., in problems using bandlimited basis functions), the reduction of computational cost based on several new properties (e.g., using ultraformulation and functions with an approach that does not necessarily imply orthogonality, differentiability or smooth continuity), the use of the Fourier transform as a fundamental design tool although the solution must be performed in the original domain (e.g., via matrix coefficients calculated by the Fourier domain), and better understanding the formulation based on the interior product as a particular case of regularization using convolution.

## **Acknowledgments**

The authors are grateful to Professor Fernando L. Teixeira of Ohio State University, USA, for participating in useful and valuable discussions. In addition, the authors would like to thank the reviewers for their constructive suggestions, which helped in improving the paper.

## **References**

- [1] A. Polyanin and A. Manzhirov, *Handbook of Integral Equations*. Boca Raton, FL, USA: CRC Press, 1998.
- [2] R. Garg, *Analytical and Computational Methods in Electromagnetics*. Boston, MA, USA: Artech House Incorporated, 2008.
- [3] M. N. O. Sadiku, *Numerical Techniques in Electromagnetics with MATLAB*, third edition. Boca Raton, FL, USA: CRC Press Inc., 2009.
- [4] R. F. Harrington, "Matrix methods for field problems," *Proceed. IEEE*, vol. 55, no. 2, pp. 136–149, Feb. 1967.
- [5] R. F. Harrington, *Field Computation by Moment Methods*. New York, NY, USA: Macmillan, 1968.
- [6] Z. Chen and S. Luo, "Generalization of the finite-difference-based time-domain methods using the method of moments," *IEEE Trans. Antennas Propag.*, vol. 54, no. 9, pp. 2515–2524, Sept. 2006. doi: 10.1109/TAP.2006.880733
- [7] Z. Chen and M. Ney, "The method of weighted residuals: A general approach to deriving time- and frequency-domain numerical methods," *IEEE Antennas Propag. Mag.*, vol. 51, no. 1, pp. 51–70, Feb. 2009. doi: 10.1109/MAP.2009.4939019
- [8] C. I. Páez, "A new computational approach to solve convolutional integral equations: The method of sampling for one dimension," Ph.D. dissertation, Univ. Andes, Bogotá, Colombia, 2017.
- [9] B. Kolundzija and B. Popovic, "Entire domain galerkin method for analysis of generalised wire antennas and scatterers," *IEE Proc. H Microw., Antennas Propaga.*, vol. 139, no. 1, pp. 17–24, Feb. 1992. doi: 10.1049/ip-h-2.1992.0004

- [10] E. Rothwell, "The transmission line as a simple example for introducing integral equations to undergraduates," *IEEE Trans. Edu.*, vol. 52, no. 4, pp. 459–469, Nov. 2009. doi: 10.1109/TE.2008.930507
- [11] G. Antonini and F. Ferranti, "Integral equation-based approach for the analysis of tapered transmission lines," *IET Sci., Meas. Technol.*, vol. 2, no. 5, pp. 295–303, Sept. 2008. doi: 10.1049/iet-smt:20070110
- [12] J. Goswami, A. Chan and C. Chui, "On solving first-kind integral equations using wavelets on a bounded interval," *IEEE Antennas Propag. Mag.*, vol. 43, no. 6, pp. 614–622, Jun. 1995. doi: 10.1109/8.387178
- [13] A. Peterson and M. Bibby, "High-order numerical solutions of the mfie for the linear dipole," *IEEE Trans. Antennas Propag.*, vol. 52, no. 10, pp. 2684–2691, Oct. 2004. doi: 10.1109/TAP.2004.834407
- [14] J. Tsalamengas, "Exponentially converging nystrom methods in scattering from infinite curved smooth strips: Part 1: Tm-case," *IEEE Trans. Antennas Propag.*, vol. 58, no. 10, pp. 3265–3274, Oct. 2010. doi: 10.1109/TAP.2010.2055788
- [15] J. Tsalamengas, "Exponentially converging nystrom methods in scattering from infinite curved smooth strips: Part 2: Te-case," *IEEE Trans. Antennas Propag.*, vol. 58, no. 10, pp. 3275–3281, Oct. 2010. doi: 10.1109/TAP.2010.2063412
- [16] O. Bucci and G. Franceschetti, "On the spatial bandwidth of scattered fields," *IEEE Trans. Antennas Propag.*, vol. 35, no. 12, pp. 1445–1455, Dec. 1987. doi: 10.1109/TAP.1987.1144024
- [17] G. Herrmann, "Note on interpolational basis functions in the method of moments [em scattering]," *IEEE Trans. Antennas Propag.*, vol. 38, no. 1, pp. 134–137, Jan. 1990. doi: 10.1109/8.43601
- [18] F. Teixeira and J. Bergmann, "Moment-method analysis of circularly symmetric reflectors using bandlimited basis functions," *IEE Proc. Microw., Antennas Propag.*, vol. 144, no. 3, pp. 179–183, Jun. 1997. doi: 10.1049/ip-map:19971109
- [19] G. Herrmann and S. Strain, "Sampling method using prefiltered band-limited green's functions for the solution of electromagnetic integral equations," *IEEE Trans. Antennas Propag.*, vol. 41, no. 1, pp. 20–24, Jan. 1993. doi: 10.1109/8.210110
- [20] J. H. Richmond, "Digital computer solutions of the rigorous equations for scattering problems," *Proc. IEEE*, vol. 53, no. 8, pp. 796–804, Aug. 1965. doi: 10.1109/PROC.1965.4057
- [21] F. N. Fritsch and R. E. Carlson, "Monotone piecewise cubic interpolation," *SIAM J. Numer. Anal.*, vol. 17, no. 2, pp. 238–246, Apr. 1980. [Online]. Available: <http://dx.doi.org/10.1137/0717021>
- [22] R. P. Brent, "Old and new algorithms for toeplitz systems," *Proc. SPIE*, vol. 0975, pp. 2–9, 1988. [Online]. Available: <http://dx.doi.org/10.1117/12.948485>
- [23] G. J. Burke, "Accuracy of reduced and extended thin-wire kernels," in *The 25th Int. Rev. Prog. Appl. Comput. Electromagn. ACES 2009*. Available: <http://bit.ly/2XY95vc>
- [24] P. Papakanellos, G. Fikioris, and A. Michalopoulou, "On the oscillations appearing in numerical solutions of solvable and nonsolvable integral equations for thin-wire antennas," *IEEE Trans. Antennas Propag.*, vol. 58, no. 5, pp. 1635–1644, May 2010. doi: 10.1109/TAP.2010.2044319

- [25] R. Allen and D. Mills, *Signal analysis*. Piscataway, NJ, USA: Wiley-IEEE Press, 2004.  
Available: <http://dsp-book.narod.ru/SATFSS1.pdf>
- [26] R. S. Strichartz, *A Guide to Distribution Theory and Fourier Transforms*. Boca Raton, FL, USA: CRC Press, 1994.

## Appendices

### A. Preliminaries

#### A.1. Standard Functions and their Characteristics

Let  $g: \mathbb{R} \rightarrow \mathbb{C}$  be a complex-valued function. Let  $g_\Omega(x)$  be a truncated function with compact support given by

$$g_\Omega(x) \triangleq \begin{cases} g(x) & \forall x \in \Omega \\ 0 & \text{otherwise} \end{cases} \quad (43)$$

Let  $\Pi_b(x) \triangleq 1_{(-b/2, b/2)}(x)$  be the rectangular function, let  $\Lambda_b(x) = (1 - |x|/b)\Pi_{2b}(x)$  be the triangular function, and let  $\text{sinc}(x) \triangleq \sin(x)/x$ .

Let  $g \in L^{1 \leq p < \infty}$  if  $\|g\|_p \triangleq \left( \int_{-\infty}^{\infty} |g(x)|^p dx \right)^{\frac{1}{p}} < \infty$ , and let  $g \in L^\infty$  if  $\|g\|_\infty \triangleq \sup_{x \in \mathbb{R}} |g(x)| < \infty$  [25]. Let  $L^{p \wedge q} = L^p \cap L^q$  and  $L^{p \vee q} = L^p \cup L^q$ .

**Definition 6.** Let  $\delta_\Delta(x)$  be a nascent Delta-Dirac function for  $g \in L^p$  if

$$\left\| g(x) - \lim_{\Delta \rightarrow 0^+} (\delta_\Delta * g)(x) \right\|_p = 0 \quad (44)$$

#### A.2. Continuous Fourier Transform

Let  $\tilde{g}(v) \triangleq \mathcal{F}\{g(x)\}$  be the *Fourier transform*. If  $g_\Omega \in L^1$ ,  $\tilde{g}^\Omega(v) \triangleq \mathcal{F}\{g_\Omega(x)\} \triangleq \int_{-\infty}^{\infty} g_\Omega(x) e^{-2\pi j xv} dx$  exists.

**Lemma 7.** (*Plancherel's theorem*) If  $g_\Omega \in L^{1 \wedge 2}$ ,  $\tilde{g}^\Omega \in L^2$  and  $\|g_\Omega(x)\|_2 = \|\tilde{g}^\Omega(v)\|_2$ .

**Definition 8.** The essential bandwidth of  $g \in L^2$  is defined by  $BW_2^g: \epsilon \triangleq 1 - \|\tilde{g}_\Theta(v)\|_2^2 / \|\tilde{g}(v)\|_2^2 \ll 1$ , where  $\Theta \triangleq (-BW_2^g, BW_2^g)$ .

### A.3. Linear System Theory

Let  $g \xrightarrow{h} f$  be a linear and invariant problem given by  $f(x) = (h * g)(x)$ , where  $g(x)$  is the input,  $f(x)$  is the output,  $h(x)$  is the linear and invariant system, and  $(*)$  is the unidimensional invariant convolution operator defined by  $(h * g)(x) = h(x) * g(x) \triangleq \int_{-\infty}^{\infty} h(x-u)g(u)du$ , in the case that the *improper Riemann integral* is well defined. Let  $\mathcal{F}\{h(x) * g(x)\} = \tilde{h}(v) \cdot \tilde{g}(v)$ , in the case that the Fourier transforms  $\tilde{h}(v) = \mathcal{F}\{h(x)\}$ ,  $\tilde{g}(v) = \mathcal{F}\{g(x)\}$  and the *improper Riemann integral* are well defined.

### A.4. Instantaneous Sampling Theory

Let  $\delta_{mn}$  be the Kronecker Delta function. Let  $\delta(x)$  be the generalized Delta Dirac function. Using the distribution theory and the generalized Fourier transform [25] and [26], the following theorems can be considered well defined:

**Lemma 9.**  $\mathcal{F}\{\delta(x - x_0)\} = e^{-2\pi j \cdot v x_0}$ ,  $\mathcal{F}\{e^{2\pi j \cdot x v_0}\} = \delta(v - v_0)$ ,  $\mathcal{F}\{\sum_{n=-\infty}^{\infty} \delta(x - n\Delta)\} = \sum_{k=-\infty}^{\infty} \Delta^{-1} \delta(v - k\Delta^{-1})$ .

**Theorem 10.** Let  $\mathcal{F}\{g(x)\} = \tilde{g}(v)$  and the uniform samples  $x_n = x_{n-1} + \Delta = x_0 + n\Delta$  with  $\vartheta = \Delta^{-1} \in \mathbb{R}$  and  $n, k \in \mathbb{Z}$ . The *ideal instantaneous sampling theorem* can be defined as

$$\mathcal{F}\left\{\sum_{n=-\infty}^{\infty} g(x_n)\delta(x - x_n)\right\} = \vartheta \cdot \sum_{k=-\infty}^{\infty} \tilde{g}(v - k\vartheta)e^{-2\pi j \cdot k\vartheta x_0} \quad (45)$$

*Proof.*  $\mathcal{F}\{\sum_{n=-\infty}^{\infty} g(x_n)\delta(x - x_n)\} = \mathcal{F}\{\sum_{n=-\infty}^{\infty} g(x_0 + n\Delta)\delta(x - x_0 - n\Delta)\} = \mathcal{F}\{\delta(x - x_0) * \sum_{n=-\infty}^{\infty} g(x_0 + n\Delta)\delta(x - n\Delta)\} = \mathcal{F}\{\delta(x - x_0) * \sum_{n=-\infty}^{\infty} g(x + x_0)\delta(x - n\Delta)\} = \mathcal{F}\{\delta(x - x_0) * (g(x + x_0) \cdot \sum_{n=-\infty}^{\infty} \delta(x - n\Delta))\} = e^{-2\pi j \cdot v x_0} \cdot ((\tilde{g}(v)e^{2\pi j \cdot v x_0}) * \sum_{k=-\infty}^{\infty} \vartheta \cdot \delta(v - k\vartheta)) = e^{-2\pi j \cdot v x_0} \cdot \sum_{k=-\infty}^{\infty} \vartheta \cdot \tilde{g}(v - k\vartheta)e^{2\pi j \cdot (v - k\vartheta)x_0} = \vartheta \cdot \sum_{k=-\infty}^{\infty} \tilde{g}(v - k\vartheta)e^{-2\pi j \cdot k\vartheta x_0}$  ■

**Theorem 11.** Let  $\mathcal{F}\{g(x)\} = \tilde{g}(v)$ ,  $\mathcal{F}\{p(x)\} = \tilde{p}(v)$  and the uniform samples  $x_n = x_{n-1} + \Delta = x_0 + n\Delta$  with  $\vartheta = \Delta^{-1} \in \mathbb{R}$  and  $n, k \in \mathbb{Z}$ . The *nonideal instantaneous sampling theorem* can be defined as

$$\mathcal{F}\left\{\sum_{n=-\infty}^{\infty} g(x_n)p(x - x_n)\right\} = \vartheta \cdot \tilde{p}(v) \cdot \sum_{k=-\infty}^{\infty} \tilde{g}(v - k\vartheta)e^{-2\pi j \cdot k\vartheta x_0} \quad (46)$$

*Proof.*  $\mathcal{F}\{\sum_{n=-\infty}^{\infty} g(x_n)p(x-x_n)\} = \mathcal{F}\{p(x) * \sum_{n=-\infty}^{\infty} g(x_n)\delta(x-x_n)\} = \vartheta \cdot \tilde{p}(\nu) \cdot \sum_{k=-\infty}^{\infty} \tilde{g}(\nu - k\vartheta)e^{-2\pi j \cdot k\vartheta x_0}$  ■

## B. Properties of Matrix B

**Corollary 12.** The matrix  $\mathbf{B} = [B_{mn}]_{N \times N} = [m - n]_{N \times N}$  for  $N \geq 3$  has a theoretical inverse given by

$$\mathbf{B}^{-1} = \frac{1}{2} \begin{bmatrix} \frac{1}{N-1} - 1 & 1 & 0 & 0 & \dots & 0 & \frac{1}{N-1} \\ 1 & -2 & 1 & 0 & \dots & 0 & 0 \\ 0 & 1 & -2 & 1 & 0 & \dots & 0 \\ \vdots & \ddots & \ddots & \ddots & \ddots & \ddots & \vdots \\ 0 & \dots & 0 & 1 & -2 & 1 & 0 \\ 0 & 0 & \dots & 0 & 1 & -2 & 1 \\ \frac{1}{N-1} & 0 & \dots & 0 & 0 & 1 & \frac{1}{N-1} - 1 \end{bmatrix} \quad (47)$$

**Corollary 13.**  $\rho^+(\mathbf{B}^{-1}) \leq 2$  for  $N \geq 3$ .